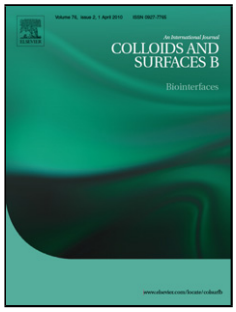

Title: Smart lipid nanoparticles containing levofloxacin and DNase for lung delivery. Design and characterization

Author: Germán A. Islan Pablo Cortez Tornello Gustavo A. Abraham Nelson Duran Guillermo R. Castro

PII: S0927-7765(16)30196-5
DOI: http://dx.doi.org/doi:10.1016/j.colsurfb.2016.03.040
Reference: COLSUB 7747

To appear in: *Colloids and Surfaces B: Biointerfaces*

Received date: 29-12-2015
Revised date: 3-3-2016
Accepted date: 14-3-2016

Please cite this article as: Germán A.Islan, Pablo Cortez Tornello, Gustavo A.Abraham, Nelson Duran, Guillermo R.Castro, Smart lipid nanoparticles containing levofloxacin and DNase for lung delivery.Design and characterization, Colloids and Surfaces B: Biointerfaces http://dx.doi.org/10.1016/j.colsurfb.2016.03.040

Smart ~~lipid~~lipid nanoparticles containing levofloxacin and DNase for lung delivery. Design and characterization

Germán A. Islan[a], Pablo Cortez Tornello[a,b], Gustavo A. Abraham[b], Nelson Duran[c,d] and Guillermo R. Castro[a *]

[a] Nanobiomaterials Laboratory, Institute of Applied Biotechnology CINDEFI (UNLP-CONICET, CCT La Plata), Dept. of Chemistry, School of Sciences, Universidad Nacional de La Plata, Calle 47y 115, La Plata 1900, Argentina.

[b] Instituto de Investigaciones en Ciencia y Tecnología de Materiales (INTEMA, Universidad Nacional de Mar del Plata, CONICET), Mar del Plata, Argentina.

[c] Institute of Chemistry, Biological Chemistry Laboratory, Universidade Estadual de Campinas, C.P. 6159, CEP 13083-970 Campinas, SP, Brazil.

[d] Brazilian Nanotechnology National Laboratory (LNNano-CNPEM), Campinas, SP, Brazil.

* Corresponding author: G. R. Castro
Tel./fax: +54 221 4833794 ext 132/103
E-mail address: grcastro@gmail.com

Graphical Abstract

Lipid nanoparticles containing levofloxacin and DNase for lung delivery.

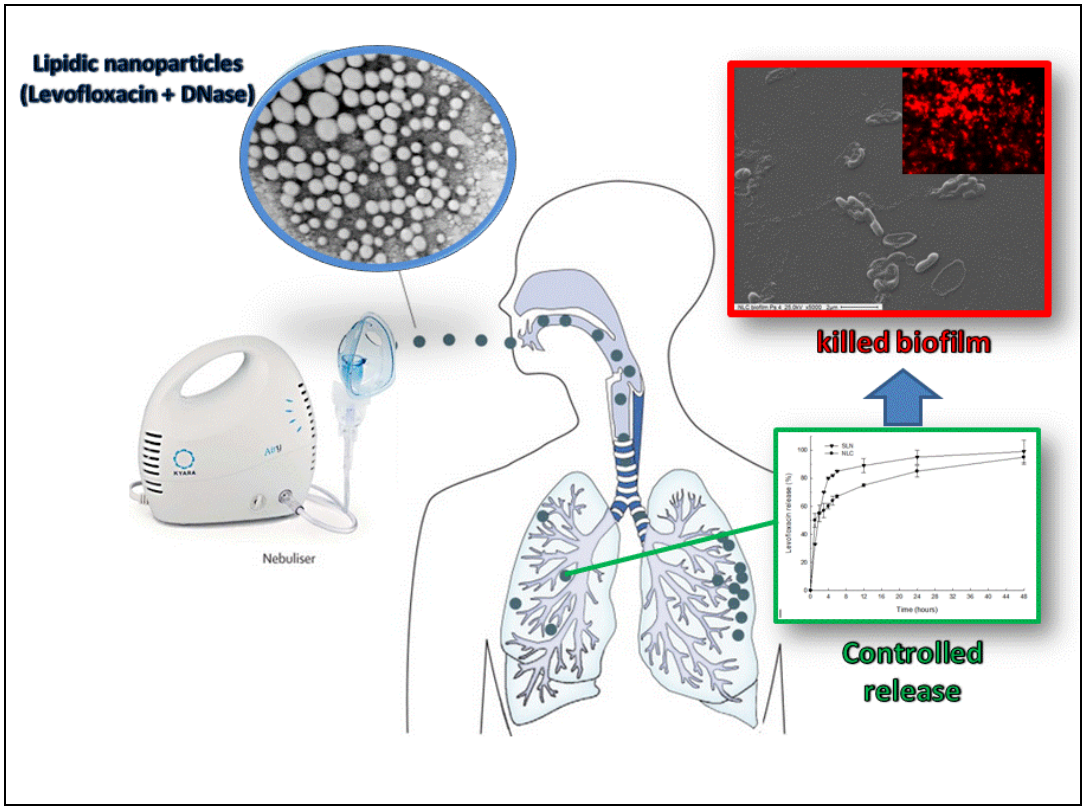

Highlights

- Levofloxacin is successfully encapsulated into lipid nanoparticles (SLN and NLCs).
- NLC formulation exhibits a controlled release profile of Levofloxacin for 2 days.
- The presence of DNase could decrease viscoelasticity found in the Cystic Fibrosis patient lungs.
- The formulation shows an active antimicrobial activity against Cystic Fibrosis pathogens.
- Lipidic nanoformulations are new alternatives for the Cystic Fibrosis treatment of infections.

Abstract

Levofloxacin (LV) is a hydrophilic ~~wide~~ broad-spectrum antibiotic commonly used in pulmonary treatment ~~of Cystic Fibrosis (CF)~~ against recurrent infections of *Pseudomonas aeruginosa*, and particularly in cystic fibrosis (CF) disease. In order to study feasible carriers for LV, solid lipid nanoparticles (SLN) of myristyl myristate were prepared by the ultrasonication method in the presence of Pluronic®F68 under different experimental conditions and characterized by dynamic light scattering, optical, transmission and scanning electron microscopy for size and morphology. Alternatively, nanostructured lipid carriers (NLCs) were developed to improve LV encapsulation and storage. SLN showed 20.1±1.4% LV encapsulation efficiency, ~~mean~~while the NLCs encapsulated 55.9±1.6% LV. NLC formulation exhibited a more controlled release profile ~~compared to~~ than SLN formulation, but both showed a biphasic drug release pattern with burst release at the first 5 hours and prolonged release afterwards, demonstrated by *in vitro* tests. The hydrodynamic average diameter and zeta potential of NLC were 182.6±3.2 nm and -10.2±0.2 mV, respectively, and were stable for at least 3 months. Additionally, DNase type I was incorporated into the formulations as a "smart" component, since the enzyme could help to decrease the viscoelasticity found in the lungs of CF patients and improves the antibiotic diffusion. FTIR, XRD, DSC, TGA and nitrogen adsorption isotherms of the nanoparticles ~~are indicating~~ indicate the presence of the loads in a noncrystalline state. The developed formulation showed an active antimicrobial activity against *Pseudomonas aeruginosa* and even against other opportunistic pathogens such as S*taphylococcus aureus*. The presence of LV-loaded NLCs reduced the formation of a bacterial biofilm, which highlighted the ~~relevance~~ significance of the nanodevice as a new alternative for ~~the~~ CF treatment.

Keywords: Levofloxacin, solid lipid nanoparticles, nanostructured lipid carriers, DNase, cystic fibrosis, pulmonary delivery.

1. Introduction

Among the illnesses with more cases of recurrent lung infections, cystic fibrosis (CF) is an inherited autosomal disease and considered one of the most common lethal genetic human disorders. It is produced by the defective function of a transmembrane conductance regulator protein, causing abnormalities in the airway physiology and mucociliary clearance [1]. These conditions are correlated with chronic lung infections recurrently ~~produced~~ caused by opportunistic pathogens, affecting more than 90% of all CF patients, and are the leading cause of morbidity and mortality [2]. Many bacterial species have been found in CF sputum, directly associated with ~~the~~ lung disease, *e.g.*, *Burkholderia cepacia*, *Haemophilus influenza* and *Staphylococcus aureus,* among others. However, *Pseudomonas aeruginosa* is considered the main cause of lethality [3]. The bacteria not only colonize lungs forming biofilms but ~~also~~ could also mutate into mucoid-type strain, thereby producing considerable amounts of ~~the~~ exopolysaccharide alginate [4]. These types of aggressive strains are capable of surviving strong antibiotic therapies and once established become extremely difficult to eradicate [5].

The progressive deterioration of lung functions in CF patients is also attributed to the airway obstruction caused by the accumulation of thick and purulent mucus. The dense secretions are mainly composed of mucus glycoproteins and DNA [6]. ~~Despite~~Although the origin of the extracellular DNA is not well established, it is suspected to be originated from necrotic neutrophils and lung tissues, ~~and a less contribution from~~ and to a lesser extent, by the contribution of infecting bacteria [7]. In addition, the alginate synthesized by the bacteria will contribute to the viscoelasticity of the mucus and drastically worsen the patient´s health when the mucoid type of *P. aeruginosa* colonizes the lungs. As a result, an early treatment of exacerbations in pulmonary symptoms as well as effective antibiotic therapies become essential tools for increasing the life expectancy and life quality of patients [8-9].

Aerosol delivery of antibiotics directly to the lungs has been proposed for the management of infections in CF patients [10]. This type of treatment increases the local concentration of the drug at the site of infection, thereby enhancing ~~the~~ its antibacterial activity and reducing the selection of resistant species compared to the outcomes of systemic administration. Currently approved CF therapies involve the use of tobramycin or aztreonam lysine solutions as inhalation agents to treat *P. aeruginosa* infections [11-12]. For several reasons, such as low drug efficacy, drug intolerance, novel emerging pathogens, and inconvenient ~~in~~ dosing, there is a real need for alternative inhaled antimicrobial therapies to treat pulmonary infections caused by *P. aeruginosa* and ~~from~~ other bacteria in CF patients [13].

Among the different vehicles for aerosol administration, solid lipid nanoparticles (SLN) have been developed in recent years as a potential system for lung delivery [14-16]. The selection of the lipid matrix is based on its properties of being nontoxic, biocompatible, of green chemical composition, physicochemical characteristics and small sizes ~~which~~ that allow them to penetrate

into almost all lung regions, enhancing the deep-lung deposition of the drugs and efficient biodistribution [17]. Many lipids were tested for the preparation of SLN, but myristyl myristate (MM) showed desirable properties as previously reported by Prof. Duran`s group such as its ability to produce SLNs using simple hot high pressure homogenization [18]. Also, MM is considered as an excellent emulsion enhancer and effective thickening ester. Particularly, MM is 100% of natural origin (*i.e.*, extracted from plants) and is present in some foods (*i.e.*, it is considered safe). In addition, it was proved that MM showed no toxicity in oral acute and dermal toxicological tests on rats. Finally, the melting point of around 40ºC is desirable for the encapsulation of a wide range of molecules, even thermolabile drugs with biological activity.

An improvement in patients' compliance due to the reduction of drug side effects in kidneys and extended drug dosing intervals due to the sustained drug release from SLNs was commonly observed [16]. In order to improve ~~the~~ SLN properties, a new generation of nanoparticles named as nanostructured lipid carriers (NLC) ~~have~~ has been developed. NLCs consist of lipid nanoparticles with liquid lipid included in their structure, ~~that~~ which decreases the crystallinity degree of the matrix. After this modification, the storage stability, the encapsulation percentage of drugs and the release profiles can be improved [~~18~~19].

In the present work, Levofloxacin (LV) ~~is used~~ has been selected as the antibiotic model for encapsulation, due to its potent activity against key pathogens in CF patients, including *P. aeruginosa*. Unlike tobramycin, LV activity is not reduced in the presence of mucus from CF sputum. Furthermore, LV has stronger antimicrobial activity than tobramycin and aztreonam in the presence of bacterial biofilms [~~19~~20]. Previous reports indicate that aerosol administration of LV is more effective in terms of plasmatic concentrations and lower inhibitory concentration ratios in the airways than those obtained with parenteral or oral administration [~~20~~21]. ~~Despite~~ Although LV is one of the safety antibiotics among the quinolone family, its use in high concentrations to reach the therapeutic levels in the lungs results in serious nephrotoxicity side effects after oral administration [~~21~~22]. The encapsulation of LV in effective therapeutic carriers for noninvasive systemic drug nanodelivery ~~becomes~~ is an interesting alternative to be explored.

~~Currently~~In the last years, LV encapsulation in SLN and NLCs has been mainly investigated for ocular delivery, but the feasibility of the carriers to transport the drug to the deepest sites of lungs is still unexplored [23]. The nanoparticles can offer a controlled release profile of the drug, prolonging the airway residence time in the lungs and preventing the emergence of resistant bacteria [~~22~~24]. Moreover, lipid nanoparticles could prevent the crystallization of the free drug at the high administered concentrations, reducing the risks of LV-induced crystal nephropathy [25]**.** ~~decreasing the dosage and the undesirable drug side effects associated with recurrent administration in patients will provide a healthier therapeutic alternative~~

~~In addition~~ It is important to mention that the incorporation of an enzyme with the ability to break down the DNA chains will improve the antibiotic ~~biodisponibility~~ bioavailability [~~23~~26-~~24~~27]. In this case, a DNase type I was incorporated into the formulation, and its effect on nanoparticle stability and activity was studied. The simultaneous presence of DNase and LV in the nanoparticles and the positive interaction between them are interesting properties that make the nanocarrier a "smart" system. DNase plays a mucolytic role in the microbial biofilm that surrounds the bacteria, enhancing the diffusion of the nanoparticles and consequently, the antimicrobial activity of fluoroquinolone. LV inhibits DNA gyrase and topoisomerase IV causing bacterial death and allowing DNase to hydrolyze all DNA material of the cells, including genomic and potential plasmids, avoiding the release of potential antibiotic resistance genes.

~~Biophysical characterizations of the formulations were carried out by spectroscopies, microscopies, thermogravimetric and light scattering analysis. Also, antimicrobial activities of the formulations were evaluated against Pseudomonas aeruginosa and Staphylococcus aureus.~~

The aims of the present study are the development of lipid nanoparticles for an efficient encapsulation of LV in the presence of DNase as mucolytic enzyme, the characterization of the system in terms of the biophysicochemical properties (spectroscopies, microscopies, thermogravimetric and light scattering analysis) and the evaluation of the antimicrobial activity against common pathogens found in pulmonary infections.

2. Materials and methods:

2.1. Materials

The lipid myristyl myristate (Crodamol™ MM, melting point = 36-40ºC) and the oil (Crodamol™ GTCC-LQ, a fully saturated emollient triester, melting point = -5ºC) were kindly donated by Croda (Argentina). Levofloxacin (LV, (S)-9-fluoro-2,3-dihydro-3-methyl-10-(4-methylpiperazin-1-yl)-7-oxo-7H-pyrido[1,2,3-de]-1,4-benzoxazine-6-carboxylic acid), deoxyribonuclease (DNase) type I from *bovine pancreas* (MW≈ 31 kDa, isoelectric point≈ 5.2), DNase test agar with toluidine blue, Pluronic®F68 (cat # A-6973) and the Live/Dead BacLight® kit were provided by Sigma–Aldrich (Buenos Aires, Argentina). *Pseudomonas aeruginosa* ATCC 15442 and *Staphylococcus aureus* ATCC 6538 were used in all antimicrobial experiments. Other reagents were of analytical grade from commercially available sources and used as received from Merck (Darmstadt, Germany) or similar ~~brand~~ suppliers.

2.2. ~~Solid lipid nanoparticles~~ SLN and ~~nanostructured lipid carrier~~ NLC preparation

SLN and NLC containing LV were prepared by the ultrasonication method [~~25~~28]. Briefly, 200 mg of lipid (1.0% w/v) ~~were~~ was melted ~~under~~ in a water bath at 60˚C and mixed with 5 mg

of LV (solid or dissolved in 100 µl of acetone). In the case of NLC, ~~liquid lipid (oil)~~ concentrations from 3.0% to 10.0% (w/w) of oil ~~was~~ were incorporated. After 10 minutes, a hot aqueous solution (20 ml) containing 1.5% (w/v) of Pluronic®F68 was added to the lipid phase. Immediately, the mixture was ultrasonicated for 50 min (40% amplitude) using an ultrasonic processor (130 Watts, Cole-Parmer, USA) equipped with a 3 mm titanium tip. Then, the dispersion was cooled at room temperature and stored at 5°C.

A stock of 10 mg/ml DNase type I was prepared in physiological solution (pH 5.0) and different volumes were added to the obtained nanodispersion to reach increasing ratios from 6.5 to 650 µg of enzyme per milligram of lipid.

2.3. Measurement of loading efficiency

The final reaction volume was measured (evaporation occurs during the sonication procedure) and the concentration of ~~free~~ nonencapsulated LV was determined. Briefly, ~~a sample of~~ 500 µl of the final dispersion were transferred to the ultrafiltration centrifugal device (MWCO= 10,000, Microcon, Millipore, Ma.) and centrifuged at 5,000 xg for 10 minutes to retain the SLNs. The filtrate was ~~ten times~~ diluted ten times in distilled water to measure the nonencapsulated LV by UV and fluorescence spectroscopy. The encapsulation efficiency (EE) was calculated as follows:

$$EE\ (\%) = \frac{(Q_0 - (Cr \times V)) \times 100}{Q_0} \qquad (1)$$

where Q_0 is the initial amount of LV, Cr is the concentration of LV in the filtered solution, and V is the final volume after finishing the preparation.

2.4. Particle size, zeta potential and polydispersion index

The mean diameter and size distribution were measured by photon correlation spectroscopy (PCS) (Nano ZS Zetasizer, Malvern Instruments Corp, UK) at 25°C in polystyrene cuvettes with a path length of 10 mm. The zeta potential was determined by laser Doppler anemometry also using the Nano ZS Zetasizer. Measurements were performed in capillary cells with path lengths of 10 mm, using deionized water obtained from a Milli-Q system. The PDI value was also determined. All the measurements were carried out in triplicate.

2.5. Physical stability

The physical stability of the nanoparticle dispersion was evaluated by examining changes of mean particle size and zeta potential during storage at 4°C protected from the light. In addition, variations in the amount of the encapsulated drug were determined.

2.6. Release studies

Molecular release experiments were performed using a dialysis membrane (MWCO 10 kDa). The membrane was soaked in distilled water for 12 hours and filled with 5 ml of each formulation, followed by immersion in 50 ml of physiological solution at pH 7.0. Every 1 hour, samples of 1.0 ml were withdrawn and LV concentration was measured at 286 nm using a UV-Vis spectrophotometer (Shimadzu, Japan). The volume withdrawn at each time was replaced by fresh medium, and the dilution was taken into account for the calculation of the drug released. All the assays were done in triplicate.

2.7. Microscopic observations

2.7.1. Optical microscopy (OM)

Optical microscopy observations of the nanoparticles were performed in a Leica DM 2500 microscope (Germany).

2.7.2. Scanning electron microscopy (SEM)

SEM studies were performed using freeze-dried samples made by sputtering their surfaces with gold (Balzers SCD 030 metalizer) with a layer thickness between 15 and 20 nm. Nanoparticle distribution and morphologies were observed using Philips SEM 505 model (Rochester, USA), and processed by an image ~~digitalizer~~ digitizer program (Soft Imaging System ADDA II (SIS)).

2.7.3. Transmission electron microscopy (TEM)

The nanoparticle dispersion was ~~ten times~~ diluted ten times with ultrapure water, and a drop of the dispersion was spread onto a collodion-coated Cu grid (400 mesh). Liquid excess was drained with filter paper. One drop of phosphotungstic acid was added to the dispersion for contrast enhancement. Finally, TEM analysis was performed using a Jeol-1200 EX II-TEM microscope (Jeol, Ma, USA).

2.8. Differential scanning calorimetry (DSC) analysis

The thermal properties of myristyl myristate, LV, DNase, and NLC, NLCL, NLCLA particles were determined by differential scanning calorimetry (DSC, PerkinElmer Inc., Model Pyris 1, Waltham, MA, USA) under nitrogen atmosphere. Scans were carried out at a heating rate of 10ºC.min^{-1} in the 0-250ºC temperature range. ~~The degree of crystallinity of myristyl mirystate (X_c) was calculated as:~~ The crystallinity variations of myristyl myristate in the nanoparticles were determined by considering the melting heat for pure myristyl myristate

(ΔHmm = 195.64 J g^{-1}), according to the equation proposed by *Freitas et al*. for a lipid concentration of 100% [29]:

$$X_C\ (\%) = (\Delta H_m experimental / \Delta H_m m) \text{ x } 100 \qquad (2)$$

~~Where $\Delta H_m m$ correspond to the melting heat for pure myristyl myristate determined on 195.64 J.g^{-1}.~~

2.9. Thermogravimetric analysis (TGA)

TGA was conducted to study the thermal stability of myristyl myristate, LV, DNase, and NLC, NLCL, NLCLA particles. TGA data were obtained using a thermogravimetric analyzer (TGA-50 Shimadzu, Japan). Then, 5–10 mg of sample was accurately weighed in an aluminum pan and the measurement was conducted at a heating rate of 10°C.min^{-1} under nitrogen purging.

2.10. X-ray diffraction (XRD)

X-ray diffraction (XRD) patterns were taken on a PANalytical X`Pert PRO diffractometer equipped with an X-ray source (Philips PW 1830, PAN analytical BV) using CuKα radiation at 40 kV and 40 mA. Diffraction patterns were collected over the 2θ range of 5°–75° with an acquisition time of 1 second at each step of 0.02°.

2.11. Attenuated total reflectance/Fourier transform infrared spectroscopy (ATR/FTIR)

Fourier transform infrared spectroscopy (FTIR) spectra were obtained by using a Nicolet 6700 (Thermo Scientific, Inc., Waltham, MA, USA) spectrometer. Attenuated total reflectance (ATR) mode was used to record spectra over the range 450–4,000 cm^{-1} at a resolution of 2 cm^{-1}.

2.12. Nitrogen adsorption isotherms

Nitrogen adsorption–desorption at 77 K at a bath temperature of -195.800°C was carried out for dried microparticles. The surface area, pore volume and pore size of the different formulations were calculated with the Micromeritics ASAP 2020V3.00 Software considering the Brunauer Emmett Teller (BET) equation or the Barrett Joyner Halenda (BJH) method.

2.13. Antimicrobial assay

Inhibition halos against *Pseudomonas aeruginosa* and *Staphylococcus aureus* were determined by using the modified disk diffusion method according to international clinical standards (CLSI/NCCLS), replacing disks for sterile glass cylinders (8x6x10 mm^3 of external and internal diameter, and length, respectively). The glass cylinders were ~~further~~ then placed on the agar plate surface inoculated with bacteria (0.5 McFarland scale). Solutions of free LV,

NLC, NLC (LV) and NLC (LV-DNase) were diluted in sterile distilled water to reach an LV concentration of 10 µg/ml. Each solution (25 µl) was placed inside the cylinders and incubated at 37°C for 24 hours. Then, inhibition zones were determined.

Additionally, *Pseudomonas aeruginosa* was grown in nutrient broth for 24 hours at 37°C. An inoculum was taken and dropped on a clean glass surface, under sterile air. Treated bacteria were placed in contact with 10 µl of the NLC formulation, ~~meanwhile~~ and untreated ones, with physiological solution. Samples were incubated for another 24 hours at 37°C to favor ~~the~~ biofilm formation. Finally, they were fixed ~~with~~ by glutaraldehyde treatment (2.5 wt%), washed with distilled water and dried with increasing concentrations of ethanol, and the culture was observed by SEM.

2.14. Staining biofilms with ~~Kit~~ the Live/Dead BacLight® kit

The commercial kit is composed of two fluorescent dyes, SYTO9® (green) and propidium iodide (red). For the microbiological assays, *P. aeruginosa* growing at late exponential phase was inoculated in a soft nutrient agar, and a drop of 20 µl was placed on the surface of a glass slide, followed by incubation for 24 hours to allow biofilm formation. Subsequently, the biofilm was covered with the NLC formulation (containing LV) for 30, 60 min and 24 hours. After treatment, the biofilms were carefully washed with deionized water.

For biofilm staining, a mixture of both dyes was prepared in equal proportions (0.75 µl of each one in 0.5 ml of sterile deionized water) and applied ~~above~~ onto the entire biofilm and held in darkness for 20 minutes. Then, the samples were washed using deionized water and observed in a Leica DM 2500 epifluorescence microscope (Germany) equipped with UV filters (495–505 nm) to determine the viability of the bacteria. The filters used were U-MWG2 (excitation between 510 and 550 nm and emission at 590 nm), which allows observing live (green) bacteria ~~with a green color~~ and U-MWB2 (excitation 460 and emission 490 520 nm), ~~with which the damaged bacteria were observed with a red color~~ which shows dead (red) bacteria.

2.15. Statistical analysis

Experiments were carried out in triplicate. Comparisons of the means were performed by analysis of variance (ANOVA) with a significance level of 5.0% ($p < 0.05$) followed by Fisher's least significant difference test at $p < 0.05$.

3. Results and discussion

3.1. Preparation of SLN and NLC for levofloxacin encapsulation

Different SLN formulations were prepared by the ultrasonication method, and the encapsulation efficiency (EE) was calculated with Equation 1 (**Table 1**). The SLN1 formulation was prepared by mixing the lipid phase with solid LV, followed by ~~and dispersion~~

homogenization in 3.0% of Pluronic F68 (dissolved in distilled water). It showed a low EE with a value around 5%, possibly due to the tendency of LV molecules to migrate towards the aqueous solution. In the SLN2, the EE was increased ~~to~~ more than ~~the double~~ twofold by adjusting the pH of the aqueous solution to 7.4 (100 mM phosphate buffer), conditions in which LV is in its neutral form and shows a reduced solubility [~~26~~30]. In the other tested formulation, SLN3, the polarities of LV molecules and the lipid phase were brought closer together by the use of acetone as solvent for LV dissolution, in such a way that the EE reached a value of 20%. ~~In a next step~~ In order to increase the amount of encapsulated LV, 3.0 wt% oil was added to the lipid phase ~~in order~~ to produce nanostructured nanoparticles [~~18~~19]. As a result, NLCs with a high encapsulation of more than 50% were obtained, ~~that~~ which can be explained considering the higher solubility of LV in a liquid lipid than in the solid lipid phase. The EE value was ~~superior compared to~~ greater than in previous reports of lipid carriers containing quinolones [~~27~~31]. The formulation was named as NLC1. Our results were in agreement with previous work in which the NLC was prepared by using 2.5% oil with an increased stability of the lipid nanoparticles [32]. Particularly, 3.0% Crodamol^{TM} GTCC-LQ oil was enough to disrupt the crystal packing structure of SLN and increase almost 3 times the EE. Finally, NLC formulations with ~~increased~~ increasing ~~oleo~~ oil concentrations showed negative effects on the LV EE, and they were discarded for next experiments. The use of 10% oil concentration in the lipid matrix showed low LV encapsulation and burst release (data not shown) compared with the developed formulations (**Table 1**).

Considering the experimental results, the NLC1 formulation was selected for the analysis of particle size, polydispersity index (PDI) and zeta potential (Z pot). The NLC1 was determined at two sonication times and in the presence or in the absence of ~~the~~ LV (~~**Table 2**~~ **Table S1**). The particle size values showed a tendency to increase the ~~particle size~~ mean diameter in the presence of the drug, suggesting its incorporation ~~inside~~ into the matrix. ~~Despite~~ A direct relationship between the sonication time and size reduction was observed up to 30 minutes ~~was commonly observed~~. However, a slight increase in the average diameter of nanoparticles by extending the sonication time was found, and it could be attributed to the ~~raise~~ rise of the solution temperature and therefore, fusion of the small nanoparticles [~~28~~33]. The Z potential (Z Pot) and PDI values were in the ranges from -8.65 to -10.3 mV and 0.302 to 0.367, respectively, indicating that the NLCs possess a negative charge surface due to the presence of negatively charged Pluronic®F68. Furthermore, the PDI range indicates that the samples were moderately polydisperse [~~29~~34].

In order to obtain more information about the NLC1 size and morphology, different microscopy techniques were employed. Optical microscopy revealed a relatively narrow distribution of the nanoparticles, which were observed as black dots at 1,000 magnifications (**Figure S1a**). SEM images of the NLC formulation were obtained, but preparation of the

sample by lyophilization induced the aggregation of nanoparticles. However, small particles can be distinguished in the diameter range of ~~the~~ 100-200 nm (**Figure S1b**). On the other hand, TEM analysis ~~allowed to observe~~ revealed the presence of clear, spherical nanoparticles ~~with spherical shape~~. The mean diameter of the NLCs was around 200 nm and in ~~concordance~~ agreement with the values found by Z-sizer measurement. Staining with phosphotungstic acid increased the contrast of the nanoparticles, so that a black shadow around the surface was observed (**Figure 1a and 1b**).

3.2. In vitro drug release

The dissolution profiles of SLN3 and NLC1 showed a biphasic behavior consisting of an initial burst release, followed by a slow release pattern (**Figure 2**). The SLN3 formulation released almost 80% of LV in the first 4 hours, ~~mean~~while the NLCs released less than 60% in the same time. This initial fast release in both cases could be attributed to the presence of free LV (non-entrapped) in the dispersion and solubilized by the surfactant micelles [35]. In addition, there was a contribution of the drug adsorbed onto the surface of nanoparticles. On the other hand, a slow release was observed afterwards, which corresponds to the drug encapsulated within the lipid matrix. The presence of amorphous LV facilitated the solubilization and release.

In fact, differences in the release patterns were observed for SLNs and NLCs. An estimation of the release rate in the slow stage ~~was~~ is shown in the inset of **Figure 2** by a linear regression (r^2 values of 0.98 and 0.94 for SLNs and NLCs, respectively). It was found that SLNs showed the slowest rate because the drug mobility is usually reduced in the solid state of solid lipids [~~18~~19]. However, an increase of more than 3 times was observed in the LV release from NLC1s, because the presence of liquid lipids within the solid lipids produced an imperfect crystal lattice of the matrix, ~~bringing~~ causing high mobility of the loaded molecules and ~~causing~~ their fast diffusion. After 12 hours, the release was more similar to that of SLN. Finally, the total drug content was released at 24 and 48 hours for SLN3s and NLC1s, respectively.

3.3. Physical stability during storage

Physical stability of the nanoparticles in solution was followed by examining changes in mean particle size and zeta potential (data not shown), but also variations in the encapsulation percentage of LV for three months (**Figure S2**). No considerable changes in the parameters were found ~~until~~ in the tested period and slight variations could be due to the polydispersity of the nanodispersion [~~30~~36]. This indicates that NLC1 formulation could be kept in a fridge (4°C) for at least three months without losing ~~of their~~ its therapeutic properties.

3.4. DNase incorporation

The feasibility of DNase incorporation into the lipid nanoparticles was a key issue for the formulation in order to improve the delivery of LV to infected lungs in CF disease. In this sense, the diffusional barrier composed of large amounts of DNA could be surpassed by enzymatic hydrolysis of the DNA molecules. Increasing ratios of DNase from *bovine pancreas* in the range of 6.5 to 650.0 μg per mg of lipid were added to the NLC1s formulation containing LV, and the effect on the mean size, Z potential and PDI of the nanoparticles was studied (**Figure S3**).

Considering that the pH of the formulation was close to 5.0, the incorporated DNase will be near its isoelectric point of 5.2, and potential interactions with hydrophobic motifs of the NLC1s structure could be established. In the present study, the mean diameter of the NLC1s increases 20 nm the size ratio after the addition of 65 μg of DNase per milligram of NLC, indicating a possible adsorption of the enzyme on the nanoparticle surface (**Figure S3a**). In ~~relationship with that~~ this regard, at the same enzyme/carrier ratio more negative Z pot values around -15 mV were obtained, suggesting an increase in NLC1 stabilization (**Figure S3b**). Although more polydispersity was observed after that point, the PDI values were under 0.35, which corresponds to particles with a medium degree of polydispersion (**Figure S3c**) [~~31~~37].

Finally, DNase activity was evaluated in a semisolid medium (DNase agar test), which is similar to the environment found in the lungs of CF patients (**Figure S3d**). The DNA degradation halos showed that the enzyme activity was unaffected after incorporation into NLCs compared with the free enzyme. The results suggest that DNase adsorption does not change the tridimensional structure of the biocatalyst. This fact is very advantageous since DNase activity will be the first agent to reduce the mucus viscosity in the lungs, increasing the antimicrobial efficiency of the antibiotic.

TEM images revealed that DNase incorporation did not change the morphology of nanoparticles, which kept their spherical shape. The nanoparticle mean diameter was around 200 nm with a medium degree of polydispersion (**Figure S4a**). Also, the NLC nanoparticles are very stable, being spherical without aggregation at 5°C for 90 days (**Figure S4b**).

3.5. Physicochemical characterization of NLCs

The porosity of the NLCs was determined by nitrogen adsorption isotherms, which ~~allow to establish~~ indicate the presence of pores in the lipid nanostructure and also ~~if~~ whether these pores could be filled by the DNase (**Figure 3**). Considering the quantity of N_2 adsorbed as a function of the relative pressure, ~~it was established~~ the presence of nanopores in the NLCs with a mean diameter of 4.2 nm was established (**Figure 3a**). Moreover, gas adsorption in the P/P_0= 0.01–0.2 range gave a specific surface area of 7.3 m²/g, calculated by the BET equation (inset in **Figure 3a**). On the other hand, the NLC formulation containing LV and DNase showed a reduction in the surface area to 3.8 m²/g, representing almost a 50% decrease of the initial value observed for empty NLCs. This result can be explained mainly by the presence of the DNase with

approximately 31 kDa MW, which coats the nanoparticle surface. In addition, the porosity analysis showed that the pore size of the NLCs did not change in the presence of the enzyme, suggesting that it was not incorporated into the lipid matrix (**Figure 3b**).

In order to obtain additional structural information, the ~~diffractograms~~ diffraction patterns of the nanoparticles ~~containing or not~~ with or without LV and DNase (abbreviated NLC, NLC-LV, and NLC-LV-A, respectively) were analyzed (**Figure 4**). LV exhibited several intense peaks at 2θ= 6.61°, 9.69°, 13.05°, 15.75°, 19.45°, 26.35°, 31.49°, and 45.37°. However, these peaks were not observed in the XRD patterns from NLC-LV and NLC-LV-A nanoparticles, suggesting that the antibiotic would be molecularly dispersed within the matrix or distributed in the lipid matrix in an amorphous state. The patterns from nanoparticles correspond to peaks of myristyl myristate (2θ= 19.11°, 21.59° and 23.29°).

The surface composition of nanoparticles was analyzed by ATR-FTIR (**Figure S5)**. Myristil myristate showed characteristic peaks at 2917 cm^{-1} and 2848 cm^{-1} (ν_a C-H and ν_s C-H in CH_2, respectively); 1735 cm^{-1} (νC=O in ester); 1463 $cm^{-1}$and 1342 cm^{-1} (δC-H in CH_2), related to ~~their~~ the ester structure. These peaks are visible in the spectra of the NLC, NLC-LV and NLC-LV-A nanoparticles. ~~Levofloxacin spectra showed their its characteristic peaks in the range of 1000 cm^{-1} to 4000 cm^{-1} as previously reported. [32]. These peaks are associated to the presence of four six membered rings with bulky groups attached at C10 and C20, displaying a third-generation fluoroquinolone structure~~. The LV FTIR spectrum showed characteristic peaks of the carboxylic group bound to the aromatic ring (peak at 3265cm^{-1}), the carbonyl group (C=O stretching vibration at 1724 cm^{-1}), the amine group (C-N stretching band at 1294 cm^{-1}) and the fluorine group (C-F stretching bands at 1084 cm^{-1}) of the molecule, which describe the distinctive chemical groups of fluoroquinolones [~~32~~38].

ATR-FTIR spectra of NLCL and NLCLA nanoparticles did not show peaks that could be associated with LV, DNase or Pluronic at the surface. ~~However, the Z potential values displayed a change in surface potential after Levofloxacin and DNase incorporation to the lipid matrix. These potential changes could be associated with the presence of small amounts of DNase on the nanoparticle surface when they are in an aqueous medium, which cannot be detected by infrared analysis of dry particles because of the low sensitivity of the FTIR technique.~~ These results suggest the incorporation of the molecules into the lipid core of nanoparticles. The small amounts of LV and DNase on the NLC surface could not be detected, probably due to the low sensitivity of the ATR-FTIR mode. However, the Z potential values previously obtained (**Table S2** and **Figure S1**) displayed a change in surface potential after LV and DNase incorporation into the lipid matrix and can be explained considering the migration of the drugs from the core of the particle surface in aqueous medium [39].

DSC and TGA techniques allowed the thermal characterization of loads and NLCs. The thermal transition of free LV, DNase, NLC, NLC-LV and NLC-LV-A ~~were~~ was determined by differential scanning calorimetry. DSC thermograms are shown in **Figure S6**, whereas the melting temperature (Tm), melting enthalpy (ΔHm) and crystallinity degree (Xc) are summarized in ~~**Table S1**~~ **Table S2**.

DSC thermograms of LV and DNase displayed a melting endotherm. These melting peaks are suppressed in NLC-LV and NLC-LV-A nanoparticles, indicating a good dispersion of amorphous LV and DNase in the NLC matrix. On the other hand, myristyl myristate crystallinity in the matrix decreased compared to plain myristyl myristate (**Table S2**). This change could be associated with the processing technique used to prepare the particles, which affects the crystallization process in many ways. Also, the formation of new amorphous regions of the matrix favors the molecular dispersion of the drug [~~33~~40].

Thermogravimetric curves of LV, DNase, myristyl myristate and NLC show a simple thermal degradation process (**Figure S7**). On the other hand, NLC-LV and NLC-LV-A nanoparticles have a complex thermal behavior. In both cases, a continuous weight loss starting at 140°C was observed, and two thermal events occurred. The first thermal event (41 wt% loss) occurred in the range of 140°C to 320°C and is related to the myristyl myristate ester. The second degradation event occurred between 320°C and 450°C with 59% weight loss, and could be ascribed to the degradation of LV and DNase. More detailed information about the weight-loss start and finish temperatures ~~of weight loss are~~ is provided in **Table S3**.

The characterizations strongly suggest that LV was included into NLCs in a noncrystalline state and was ~~feasible to be~~ likely dissolved in the environment, in agreement with previous release assays (**Figure 2**).

3.6. Antimicrobial assays

The antimicrobial activity of LV-loaded NLC1s was tested against two opportunistic pathogens commonly associated with CF disease: *Pseudomonas aeruginosa* and *Staphylococcus aureus* (**Figure 5**). The same inhibition halo was observed in the case of NLC-LV and NLC-LV-A (containing DNase) in both strains, indicating that the presence of the enzyme is not interfering with the antibiotic activity under the tested conditions. However, ~~it was expected~~ an increase of the antibiotic diffusion in the CF lung conditions, where the viscous mucus medium was mainly composed of DNA, was expected. A 10% reduction in the inhibition halo was observed for the NLC-LV formulations compared with free LV, due to the decrease of the LV diffusional rate in the encapsulated antibiotic (**Figure 5a and 5b**). An approach to the seeding zone of empty NLCs revealed that *Staphylococcus aureus* was more susceptible to inhibition than *Pseudomonas aeruginosa,* which may be due to the presence of the NLC surfactant that is affecting the cell membrane stability.

Finally, the ability of the NLC-LV-A to reduce biofilm formation was determined in *Pseudomonas aeruginosa*, the most important mucoid bacteria in the complications of CF pathologies (**Figure 6**). The bacteria were able to produce a dense biofilm after 12 hours, as was shown by SEM images (**Figure 6a**). A mix of death and live bacteria ~~were~~ was immersed in an exopolysaccharide matrix, mainly composed of alginate [5]. After treatment with NLC-LV-A, a clear antimicrobial effect was observed and the biofilm was totally disrupted (**Figure 6b**). Collapsed bacteria, membrane damage and cellular debris were observed after treatment.

In order to determine the time dependence of the biofilm integrity after treatment with the NLC formulation, the viability of the bacteria ~~were~~ was tested with the Live/Dead BacLight® kit (**Figure 7**). The untreated biofilm was mainly composed of live bacteria, which were green-stained. However, after a 30-minute ~~exposition~~ exposure to NLC-LV-A formulation, a red population began to appear, indicating the presence of damaged bacteria with loss of membrane integrity. One hour later, only few green bacteria were observed in comparison with red ones, which suggested an important damage of the bacteria immersed in the biofilm after treatment. After 24 hours with NLCs, all bacteria were red-stained due to the antimicrobial activity of LV-loaded nanoparticles.

4. Conclusions

In the present work, novel solid lipid nanoparticles (SLN) and nanostructured lipid carriers (NLCs) containing LV were successfully prepared and characterized. A DNase was also incorporated into the formulations, and its relevant activity can be associated with a decrease in the mucus viscoelasticity found in the CF patients' lungs, ~~and therefore improving~~ which improves the antibiotic diffusion. The preparation of nanoparticles can be tailored by changing the pH of the aqueous environment, the dissolution kinetics of the antibiotic in the lipid phase or the nanostructuration of the matrix by the addition of oil. Consequently, different encapsulation percentages were obtained in the range from 5% to 56 %. A good matching between the DLS results and TEM images ~~were~~ was observed, since SLNs and NLCs seem to be spherically with an average diameter of 200 nm and narrow size distribution. Lipid nanoparticles showed a controlled release of LV for at least two days, which is advantageous to reduce the high antibiotic concentrations and represents a reduction in dose enhancing the patient's comfort. The formulation could be ~~storage~~ stored ~~for~~ at 5°C for at least 3 months without changes in ~~their~~ its macroscopic properties and antimicrobial activities. Characterization of the formulation by FTIR, XRD, DSC and TGA revealed the presence of the antibiotic inside the nanoparticles and suggested the attachment of the DNase onto the surface. In addition, both components were in a noncrystalline state. Lipid nanoparticles showed a strong antibacterial activity against the gram-positive and gram-negative microorganisms tested. Also, they were able to destroy biofilms of

Pseudomonas aeruginosa strain, the most relevant pathogen in the compliance of CF disease patients.

The dual capability of nanoparticles to simultaneously deliver an antibiotic and a hydrolytic enzyme of DNA is an interesting "smart" feature to reduce the biofilm formation of the bacteria and increase antimicrobial activity, which highlights the importance of this nanosystem as a new alternative to improve the current CF therapy against infections. Similar approaches were previously developed in our laboratory using microspheres loaded with ciprofloxacin and alginate lyase (i.e., a hydrolytic enzyme of alginate) [41-42]. Also, the use of nanoparticles as effective carriers to overcome the mucus barrier for lung delivery of DNA in gene therapy or for antibiotic therapy has been reported [16-43]. The encapsulation of quinolones in SLN for ocular therapies has also been published [44]. To the best of our knowledge, this is the first report of the LV-DNase system inside solid lipid nanoparticles with special application in lung delivery. ~~Present~~Further studies are ~~carrying~~ being carried out to ~~adequate~~ adjust the formulations in order to provide better therapeutic effects in animal models and test the mucoadhesive/mucopenetration potential of these nanocarriers.

Acknowledgements

The present work was supported by Argentine grants from CONICET (National Council for Science and Technology, PIP 0498), The National Agency of Scientific and Technological Promotion (ANPCyT, PICT 2011-2116), *Fundación Argentina de Nanotecnología,* UNLP (National University of La Plata, 11/X545 and PRH 5.2). Dr. G.A. Islan thanks the "Grant for Young Researchers from UNLP 2014" and the "Program for academic mobility at teaching scale from AUGM" for financing some reagents used in the present work and the travel allowance to stay in Prof. Duran's laboratory. Also, we want to thank CRODA Argentina for kindly donating the lipids. Support from the Brazilian Network on Nanotoxicology (MCTI/CNPq) and NanoBioss (MCTI)-Brazil is also acknowledged. We also appreciate the initial collaboration and suggestions from Dr. P.D. Marcato, during her ~~posdoctorate~~ postdoctoral studies in our institution.

References

[1] Cutting, G. R. (2015). Cystic fibrosis genetics: from molecular understanding to clinical application. *Nature Reviews Genetics*, 16(1), 45-56.

[2] Stoltz, D. A., Meyerholz, D. K., & Welsh, M. J. (2015). Origins of cystic fibrosis lung disease. *New England Journal of Medicine*, 372(4), 351-362.

[3] Folkesson, A., Jelsbak, L., Yang, L., Johansen, H. K., Ciofu, O., Høiby, N., & Molin, S. (2012). Adaptation of *Pseudomonas aeruginosa* to the cystic fibrosis airway: an evolutionary perspective. *Nature Reviews Microbiology*, 10(12), 841-851.

[4] Ciofu, O., Mandsberg, L. F., Wang, H., & Høiby, N. (2012). Phenotypes selected during chronic lung infection in cystic fibrosis patients: implications for the treatment of Pseudomonas aeruginosa biofilm infections. *FEMS Immunology & Medical Microbiology*, 65(2), 215-225.

[5] Hodges, N. A., & Gordon, C. A. (1991). Protection of *Pseudomonas aeruginosa* against ciprofloxacin and beta-lactams by homologous alginate. *Antimicrobial Agents and Chemotherapy*, 35(11), 2450-2452.

[6] Lethem, M., James, S. L., Marriott, C., & Burke, J. F. (1990). The origin of DNA associated with mucus glycoproteins in cystic fibrosis sputum. *European Respiratory Journal*, 3(1), 19-23.

[7] Papayannopoulos, V., Staab, D., & Zychlinsky, A. (2011). Neutrophil elastase enhances sputum solubilization in cystic fibrosis patients receiving DNase therapy. *PloS one*, *6*(12), e28526.

[8] Ratjen, F., Döring, G., & Nikolaizik, W. H. (2001). Effect of inhaled tobramycin on early Pseudomonas aeruginosa colonisation in patients with cystic fibrosis. *The Lancet*, 358(9286), 983-984.

[9] Gibson, R. L., Emerson, J., Mayer-Hamblett, N., Burns, J. L., McNamara, S., Accurso, F. J., & Ramsey, B. W. (2007). Duration of treatment effect after tobramycin solution for inhalation in young children with cystic fibrosis. *Pediatric Pulmonology*, 42(7), 610-623.

[10] Kesser, K. C., & Geller, D. E. (2009). New aerosol delivery devices for cystic fibrosis. *Respiratory care*, 54(6), 754-768.

[11] Rose, L. M., & Neale, R. (2010). Development of the first inhaled antibiotic for the treatment of cystic fibrosis. *Science Translational Medicine*, 2(63), 63mr4.

[12] Pesaturo, K. A., Horton, E. R., & Belliveau, P. (2012). Inhaled aztreonam lysine for cystic fibrosis pulmonary disease–related outcomes. *Annals of Pharmacotherapy*, 46(7-8), 1076-1085.

[13] Döring, G., Flume, P., Heijerman, H., Elborn, J. S., & Consensus Study Group. (2012). Treatment of lung infection in patients with cystic fibrosis: current and future strategies. *Journal of Cystic Fibrosis*, 11(6), 461-479.

[14] Jaspart, S., Bertholet, P., Piel, G., Dogné, J. M., Delattre, L., & Evrard, B. (2007). Solid lipid microparticles as a sustained release system for pulmonary drug delivery. *European Journal of Pharmaceutics and Biopharmaceutics*, 65(1), 47-56.

[15] Liu, J., Gong, T., Fu, H., Wang, C., Wang, X., Chen, Q., & Zhang, Z. (2008). Solid lipid nanoparticles for pulmonary delivery of insulin. *International Journal of Pharmaceutics*, 356(1), 333-344

[16] Varshosaz, J., Ghaffari, S., Mirshojaei, S. F., Jafarian, A., Atyabi, F., Kobarfard, F., & Azarmi, S. (2013). Biodistribution of amikacin solid lipid nanoparticles after pulmonary delivery. *BioMed Research International*, Article ID 136859, 8 pages. doi:10.1155/2013/136859

[17] Nafee, N., Husari, A., Maurer, C. K., Lu, C., de Rossi, C., Steinbach, A., Hartmann R. W., Lehr, C.M. & Schneider, M. (2014). Antibiotic-free nanotherapeutics: Ultra-small, mucus-penetrating solid lipid nanoparticles enhance the pulmonary delivery and anti-virulence efficacy of novel quorum sensing inhibitors. *Journal of Controlled Release*, 192, 131-140.

[18] Ridolfi, D. M., Marcato, P. D., Justo, G. Z., Cordi, L., Machado, D., Durán, N. (2012). Chitosan-solid lipid nanoparticles as carriers for topical delivery of tretinoin. Colloids and Surfaces B: Biointerfaces, 93, 36-40.

[~~18~~19] Fang, C. L., A Al-Suwayeh, S., & Fang, J. Y. (2013). Nanostructured lipid carriers (NLCs) for drug delivery and targeting. *Recent Patents on Nanotechnology*, 7(1), 41-55.

[~~19~~20] Geller, D. E., Flume, P. A., Griffith, D. C., Morgan, E., White, D., Loutit, J. S., & Dudley, M. N. (2011). Pharmacokinetics and safety of MP-376 (Levofloxacin inhalation solution) in cystic fibrosis subjects. *Antimicrobial agents and chemotherapy*, 55(6), 2636-2640.

[~~20~~21] Döring, G., & Dalhoff, A. (2013). Aerosolised LVfloxacin in cystic fibrosis. *Expert Opinion on Orphan Drugs*, 1(7), 549-556.

[~~21~~22] Carbon, C. (2001). Comparison of side effects of LVfloxacin versus other fluoroquinolones. *hemotherapy*, 47(Suppl. 3), 9-14.

[23] Baig, M. S., Ahad, A., Aslam, M., Imam, S. S., Aqil, M., & Ali, A. (2016). Application of Box–Behnken design for preparation of levofloxacin-loaded stearic acid solid lipid nanoparticles for ocular delivery: Optimization, in vitro release, ocular tolerance, and antibacterial activity. *International Journal of Biological Macromolecules 85*, 258-270.

[~~22~~24] Suk, J. S., Lai, S. K., Wang, Y. Y., Ensign, L. M., Zeitlin, P. L., Boyle, M. P., & Hanes, J. (2009). The penetration of fresh undiluted sputum expectorated by cystic fibrosis patients by non-adhesive polymer nanoparticles. *Biomaterials*, 30(13), 2591-2597.

[25] Liu Y, He Q, Wu M. (2015). Levofloxacin-induced crystal nephropathy. *Nephrology (Carlton)* 20, 437-438.

[~~23~~26] Ratjen, F., Paul, K., Van Koningsbruggen, S., Breitenstein, S., Rietschel, E., & Nikolaizik, W. (2005). DNA concentrations in BAL fluid of cystic fibrosis patients with early lung disease: influence of treatment with dornase alpha. *Pediatric Pulmonology*, 39(1), 1-4.

[~~24~~27] Alipour, M., Suntres, Z. E., & Omri, A. (2009). Importance of DNase and alginate lyase for enhancing free and liposome encapsulated aminoglycoside activity against *Pseudomonas aeruginosa*. *Journal of Antimicrobial Chemotherapy*, 64(2):317-25.

[~~25~~28] Venkateswarlu, V., & Manjunath, K. (2004). Preparation, characterization and in vitro release kinetics of clozapine solid lipid nanoparticles. *Journal of Controlled Release*, 95(3), 627-638.

[29] Freitas, C., Müller, R.H. (1999). Correlation between long-term stability of solid lipid nanoparticles (SLN) and crystallinity of the lipid phase. *Eur. J. Pharm. Biopharm.* 47, 125–132.

[~~26~~30] North, D. S., Fish, D. N., & Redington, J. J. (1998). Levofloxacin, a second-generation fluoroquinolone. *Pharmacotherapy: The Journal of Human Pharmacology and Drug Therapy*, 18(5), 915-935.

[~~27~~31] Shah, M., Agrawal, Y. K., Garala, K., & Ramkishan, A. (2012). Solid lipid nanoparticles of a water soluble drug, ciprofloxacin hydrochloride. *Indian Journal of Pharmaceutical Sciences*, 74(5), 434.

[32] Yang, Y., Corona, A., Schubert, B., Reeder, R., & Henson, M. A. (2014).The effect of oil type on the aggregation stability of nanostructured lipid carriers. *Journal of colloid and interface science*, *418*, 261-272.

[~~28~~33] Siddiqui, A., Alayoubi, A., El-Malah, Y., & Nazzal, S. (2014). Modeling the effect of sonication parameters on size and dispersion temperature of solid lipid nanoparticles (SLNs) by response surface methodology (RSM). *Pharmaceutical Development and Technology*, 19(3), 342-346.

[~~29~~34] Schärtl, W. (2007). *Light scattering from polymer solutions and nanoparticle dispersions*. Springer Science & Business Media.

[35] Bhardwaj, V., Bhardwaj, T., Sharma, K., Gupta, A., Chauhan, S., Cameotra, S. S., Sharma, S., Gupta, R. & Sharma, P. (2014). Drug–surfactant interaction: thermo-acoustic investigation of sodium dodecyl sulfate and antimicrobial drug (levofloxacin) for potential pharmaceutical application. *RSC Advances* 4, 24935-24943.

[~~30~~36] Guterres, S. S., Alves, M. P., & Pohlmann, A. R. (2007). Polymeric nanoparticles, nanospheres and nanocapsules, for cutaneous applications. *Drug Target Insights*, 2, 147.

[~~31~~37] Wolgang, S. (2007). Sample preparation in light scattering from polymer solution and nanoparticle dispersions. 43-44, Springer Berlin Heidelberg GmbH & Co. K.

[~~32~~38] Gunasekaran S, K. Rajalakshmi , S. Kumaresan. Vibrational analysis, electronic structure and nonlinear optical properties of LVfloxacin by density functional theory. *Spectrochimica Acta Part A*: *Molecular and Biomolecular Spectroscopy* 112 (2013) 351–363.

[39] Honary, S., & Zahir, F. (2013). Effect of zeta potential on the properties of nano-drug delivery systems-a review (Part 2). Tropical Journal of Pharmaceutical Research 12: 265-273.

[~~33~~40] Singh KK, Pople PV. Development and evaluation of topical formulation containing solid lipid nanoparticles of vitamin A. *AAPS Pharm Sci Tech*. 2006;7(4):E63–9.

[41] Islan, G. A., Bosio, V. E., & Castro, G. R. (2013). Alginate lyase and ciprofloxacin co-immobilization on biopolymeric microspheres for cystic fibrosis treatment. *Macromolecular bioscience*, *13*, 1238-1248.

[42] Islan, G.A., Martinez, Y.N., Illanes, A., & Castro, G.R. (2014). Development of novel alginate lyase cross-linked aggregates for the oral treatment of cystic fibrosis. *RSC Advances*, *4*, 11758-11765.

[43] Suk, J.S., Kim, A.J., Trehan, K., Schneider, C.S., Cebotaru, L., Woodward, O.M., Boylan, N. J., Boyle, M.P., Lai, S.K., Guggino, W.B. & Hanes, J. (2014). Lung gene therapy with highly compacted DNA nanoparticles that overcome the mucus barrier. *Journal of Controlled Release*, *178*, 8-17.

[44] Kalam, M.A., Sultana, Y., Ali, A., Aqil, M., Mishra, A.K., & Chuttani, K. (2010). Preparation, characterization, and evaluation of gatifloxacin loaded solid lipid nanoparticles as colloidal ocular drug delivery system. *Journal of drug targeting*, *18*, 191-204.

Figures

Figure 1 TEM images of Levofloxacin loaded NLCs at different scale (a-b). Nanoparticles are dyed with phosphotungstic acid to enhance the contrast.

Figure 2 Release profiles of Levofloxacin from SLN and NLC formulation (4.0 µg/ml of initial LV). Inset shows the initial release from each type of nanoparticles. Errors: SD, n= 3.

Figure 3 Nitrogen adsorption–desorption isotherms of NLC (a) and NLC-LV-A (DNase) formulation (b). The insets refer to the BET specific surface area analysis. Filled and open circles refer to adsorption and desorption isotherms.

Figure 4 XRD patterns of Levofloxacin, DNase, and NLC, NLC-LV, NLC-LV-A nanoparticles.

Figure 5 Antimicrobial assays of free LV, NLC, NLC (LV) and NLC (LV-DNase) formulations. Inhibition halos are observed against *Pseudomonas aeruginosa* (a) and *Staphylococcus aureus* (b).

Figure 6 SEM images of the bactericidal and anti-biofilm formation produced by treatment of *Pseudomonas aeruginosa* with the NLC (LV-DNase) formulations. a) untreated bacteria with a clear biofilm formation and b) treated bacteria at 5,000X magnification.

Figure 7. *Pseudomonas aeruginosa* biofilm dyed with the LIVE/DEAD BacLight® kit and observed at epifluorescent microscope at 400X. Overlay images of untreated biofilm (a) and biofilm after treatment with NLC formulation for 60 min (b).

Figure 1

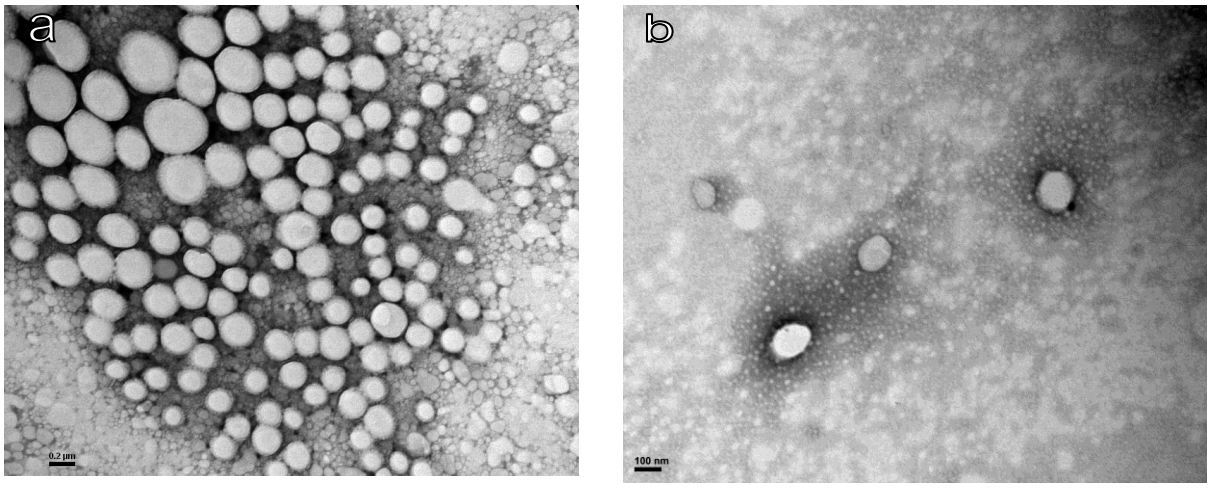

Figure 2

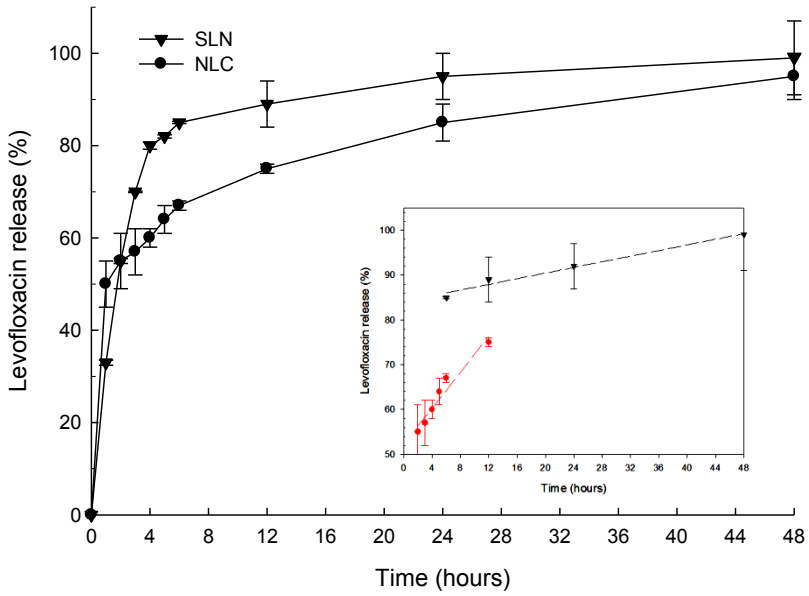

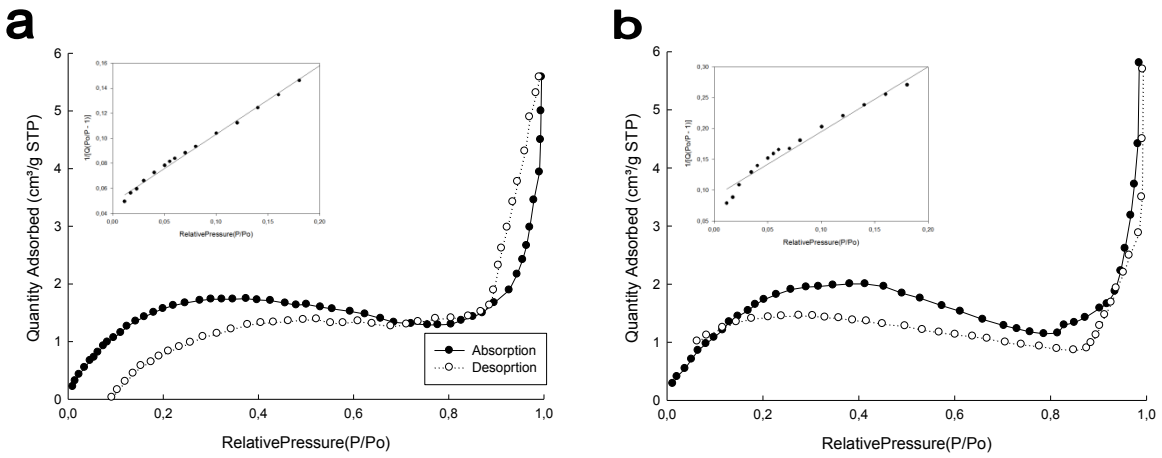

Figure 3

Figure 4

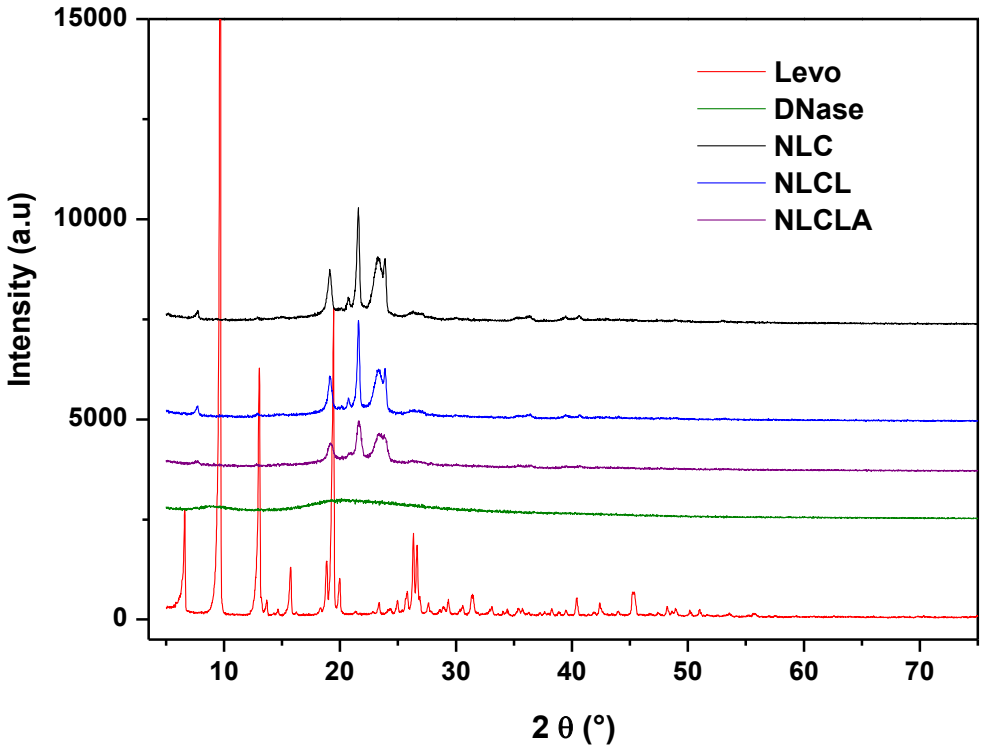

Figure 5

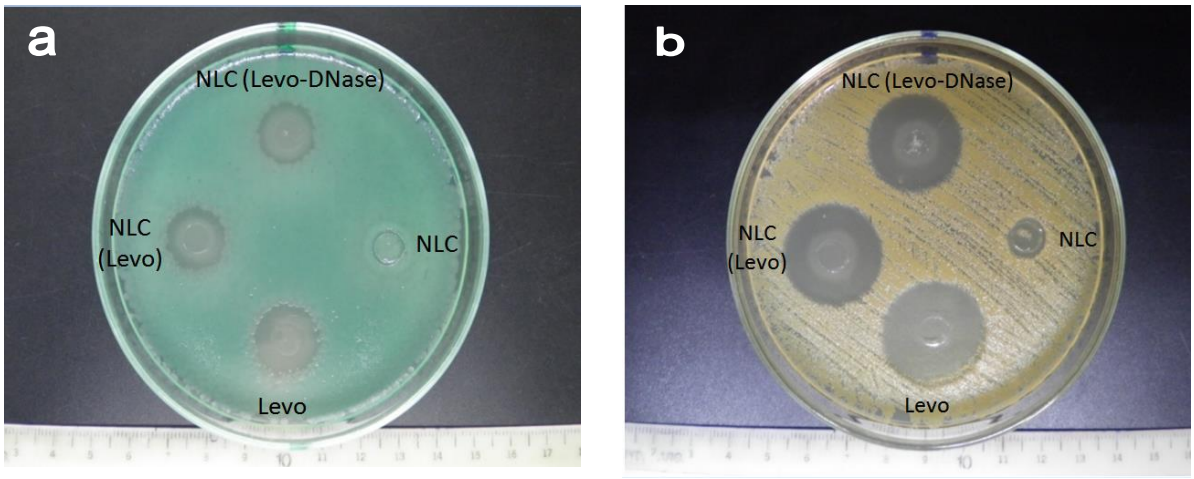

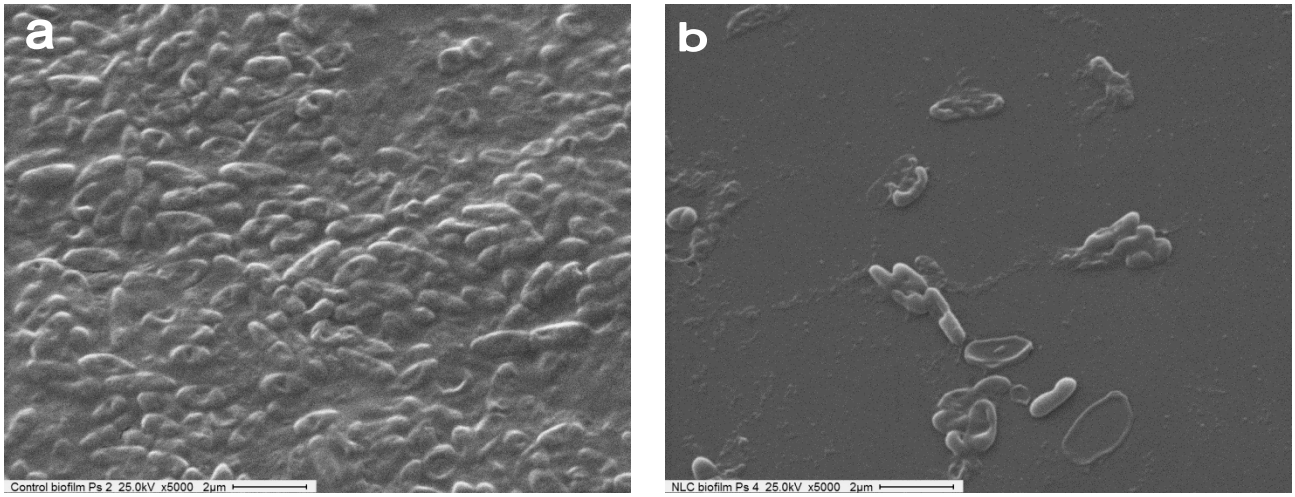

Figure 6

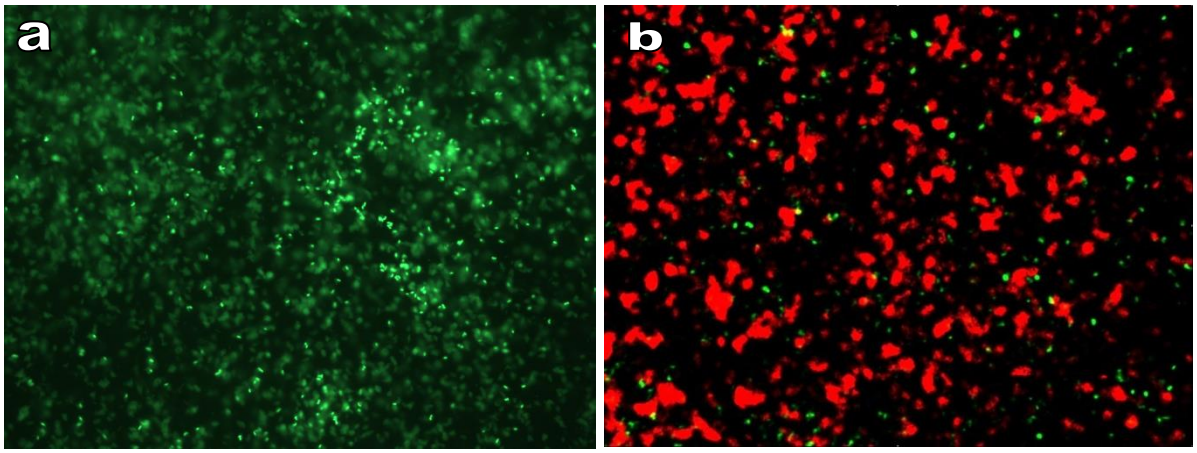

Figure 7

TABLE

Table 1. Different Solid lipid nanoparticles (SLN) and Nanostructured lipid carrier (NLC) formulations for Levofloxacin incorporation by sonication method. Composition and encapsulation efficiency (EE).

Sample	**Aqueous phase**[1]	**Hydrophobic phase**			**EE (%)**	**Mass LV/lipid (µg/mg)**
		Lipid (g)	Oil (wt%)	LV (mg)[2]		
SLN1	distilled water	0.2	-	5.0 (solid)	5.2 ±1.9	1.3
SLN2	PBS 100 mM pH=7.4	0.2	-	5.0 (solid)	12.5 ±0.4	3.1
SLN3	PBS 100 mM pH=7.4	0.2	-	5.0 (acetone)	20.1 ±1.4	5.0
NLC1	PBS 100 mM pH=7.4	0.2	3.0	5.0 (acetone)	55.9 ±1.6	14.0
NLC2	PBS 100 mM pH=7.4	0.2	10.0	5.0 (acetone)	12.2 ±1.6	3.1

Obs.: SD, n= 3; [1] Containing Pluronic®F68 at 3.0 wt%; [2] Solid or dissolved in 100 µl of acetone.